Compact and Stable Modeling of Partial Inductance and Reluctance Matrices

Hong Li, Venkataramanan Balakrishnan, Cheng-Kok Koh
School of Electrical and Computer Engineering
Purdue University, West Lafayette, IN 47907-2035
E-mail: {li73, ragu, chengkok}@purdue.edu

Guoan Zhong
Magma Design Automation
5460 Bayfront Plaza, Santa Clara, CA 95054
E-mail: gzhong@Magma-DA.com

Abstract— **The sparsification of the reluctance matrix L^{-1} (where L denotes the usual inductance matrix L) has been widely used in several recent investigations to make the problem of simulation of interconnects tractable. Although these sparsification techniques work well in practice, the stability of these approximations has not been established, i.e., the sparsified reluctance and inductance matrices are not guaranteed to be positive-definite. In this work, we propose a band matching method that enjoys two advantages: First, we exploit the elegant structure of the inverse of banded matrices so as to construct an approximate inductance matrix $\tilde{L}$ whose band entries match the band entries of original L, and whose inverse is a banded matrix. This approach yields a *compact* representation of both inductance and reluctance matrices. Second, we establish that the compact approximant $\tilde{L}$ is *guaranteed to be positive-definite*. Simulation results show that our approach enjoys an approximation accuracy that is comparable to that of existing methods.**

I. Introduction

With the aggressive scaling of VLSI technology, the problem of accurate modeling of interconnects has become increasingly important. The Partial Element Equivalent Circuit (PEEC) model has been widely used to analyze on-chip interconnects [13]. However the (partial) inductance matrix L [12] obtained from the PEEC model is large and dense. Using L directly in the simulation of interconnects typically places unrealistic demands on both simulation time and memory. A standard approach to address this issue is that of sparsification of L. Another, more recent, approach involves the sparsification of the (partial) reluctance matrix L^{-1} (rather than directly sparsifying L) [9], [6], [5], [7], [2], [3], [4], [16].

The direct truncation of L, i.e., setting to zero off-diagonal terms that are smaller in magnitude than a threshold, may result in an approximate inductance matrix that is not positive-definite, with the consequence that the simulation is unstable. An alternative to simple truncation, the shift-truncate method method proposed in [9], [6], can guarantee that the approximate inductance matrix is positive definite; however, this comes at a cost of loss of accuracy [5], [7]. Devgan *et al.* [5], noting that the off-diagonal entries of L^{-1} diminish much faster than those in L, proposed the sparsification of L^{-1}, the reluctance matrix. The resulting truncated L^{-1} (denoted as $\bar{L}^{-1}$) can reduce the number of coupling terms and speed up the simulation. However, L^{-1} needs to computed first, which is prohibitively expensive. Several window-based techniques have been used to approximate $\bar{L}^{-1}$ [7], [3], [4]. In such techniques, a small inductance sub-matrix of wires strongly coupled to the wire of interest is inverted, and the corresponding row (or column) of the wire of interest in the inverse forms the significant entries in the approximate matrix (denoted as $\hat{L}^{-1}$). While sparsification of the reluctance matrix offers better simulation accuracy than the direct sparsification of L, we note that stability of the approximation is not guaranteed with this approach either.

In [7], [4], special-purpose simulation tools that can handle reluctance elements directly have been developed. To avoid the reluctance element in simulation, the approximate reluctance matrix ($\bar{L}^{-1}$ or $\hat{L}^{-1}$) can be inverted to obtain a new dense inductance matrix, which is again not suitable for efficient simulation. The approach used in [2] is to further sparsify the matrix $\bar{L}$: By using exponential potentials, the sparsified $\bar{L}$ matrix can be calculated directly [3]. A second approach is the wire duplication method proposed in [16] that constructs, in the inductance domain, a circuit that is equivalent to a sparse reluctance matrix for the efficient simulation of reluctance elements. It has also been shown in [10], [15], [8] that representing a reluctance matrix with an equivalent circuit that consists of only resistors and controlled voltage and current sources can also speed up its simulation tremendously.

In summary, it is fair to say that most recent efforts in the modeling, analysis, and simulation of on-chip interconnects have largely been driven by the sparsification of L^{-1}, owing to the better simulation accuracy obtained as compared with the direct sparsification of L. However, the stability of these sparsification techniques has not been established; the sparsified L and L^{-1} matrices may not be positive definite.

In this work we present a band matching method for the approximation of the inductance matrix for n aligned parallel wires in a single layer. The band entries of the approximate inductance matrix, denoted as $\tilde{L}$, match those of L. Our model has several advantages: (i) $\tilde{L}^{-1}$ is sparse. (ii) $\tilde{L}$ preserves stability, i.e., it is guaranteed to be positive definite. (iii) Not only can $\tilde{L}^{-1}$ be modeled compactly, it takes only $O(n)$ parameters to model $\tilde{L}$, and $O(n)$ operations to compute it. (iv) Perhaps less significant, the physical interpretation of the entries of the inductance matrix within the remains intact. Simulation results show that the proposed model is highly accurate.

II. Compact modeling: A simple example

In [16] it has been observed that a dense matrix whose inverse is banded contains redundant information. If A is a $n \times n$ banded matrix with bandwidth $2b+1$ and $B = A^{-1}$, the significant entries of A can be computed by using only a subset of the matrix B. We take the intersection of rows $i-b$ to $i+b$ and columns $i-b$ to $i+b$ of B to form a sub-matrix. Then, the center row and center column of the inverse of the sub-matrix are identical

to the ith row and ith column of the A matrix:

$$A(i,i-b:i+b) = (B(i-b:i+b,i-b:i+b))^{-1}(b+1,:),$$
$$A(i-b:i+b,i) = (B(i-b:i+b,i-b:i+b))^{-1}(:,b+1). \quad (1)$$

Here, $A(i:j,m:n)$ refers to the sub-matrix at the intersection of rows i to j and columns m to n of A, $A(:,m)$ refers to column m and $A(i,:)$ refers to row i.

We shall reveal in this section that not only does B contain redundant information, it has an elegant structure that leads to a compact model.

Consider for example a dense symmetric matrix B, whose inverse is tridiagonal. We can obtain B^{-1} by using only the band entries of B. Using such an approach, only $3n-2$ entries of B are required to compute B^{-1}. However, all the $n(n+1)/2$ entries would be required if we were to invert the B directly. Therefore, we can conclude that at most $3n-2$ entries of B are independent. The remaining entries of B can be derived from these independent entries. Moreover, B^{-1} has only $2n-1$ significant entries. It would appear that even the $3n-2$ band entries of B contain redundancy.

Indeed, we shall now show that only $2n-1$ parameters are required to describe B. First, we introduce the following lemma, which is from [11]:

Lemma II.1: ([11]) Let $A \in R^{n,n}$ be a symmetric, irreducible, and nonsingular matrix. A is tridiagonal if and only if $B = [b_{i,j}] = A^{-1}$ is given by two sequences of numbers such that

$$B = \begin{pmatrix} u_1v_1 & u_1v_2 & \cdots & u_1v_n \\ u_1v_2 & u_2v_2 & \cdots & u_2v_n \\ \vdots & \vdots & \ddots & \vdots \\ u_1v_n & u_2v_n & \cdots & u_nv_n \end{pmatrix}, \text{ or } b_{i,j} = \begin{cases} u_iv_j & i \le j; \\ u_jv_i & i \ge j. \end{cases} \quad (2)$$

A more elegant way to describe B is to represent it as the Hadamard product of two matrices, which is defined as follows:

Definition 1: The Hadamard product of $X = [x_{i,j}]$ and $Y = [y_{i,j}]$ is defined by $X \circ Y = [x_{i,j} \times y_{i,j}]$.

Hence, matrices of the form in (2) can be written as

$$B = \underbrace{\begin{pmatrix} u_1 & u_1 & \cdots & u_1 \\ u_1 & u_2 & \cdots & u_2 \\ \vdots & \vdots & \ddots & \vdots \\ u_1 & u_2 & \cdots & u_n \end{pmatrix}}_{U} \circ \underbrace{\begin{pmatrix} v_1 & v_2 & \cdots & v_n \\ v_2 & v_2 & \cdots & v_n \\ \vdots & \vdots & \ddots & \vdots \\ v_n & v_n & \cdots & v_n \end{pmatrix}}_{V}, \quad (3)$$

where the matrices U and V form so-called "type D" and "flipped type D" matrices respectively.

Given B, whose inverse is tridiagonal, we can compute a series of parameters $\{u_i\}_{i=1}^n$ and $\{v_i\}_{i=1}^n$ as follows:

$$u_1 = 1, \quad u_i = \frac{b_{i,i}}{b_{i-1,i}}u_{i-1}, \quad v_1 = b_{1,1}, \quad v_i = \frac{b_{i-1,i}}{u_{i-1}}. \quad (4)$$

Only the tridiagonal entries of B are required for the calculation of $\{u_i\}_{i=1}^n$ and $\{v_i\}_{i=1}^n$. In other words, B can be compactly described by $2n-1$ parameters, and the parameterization of B can be performed with $O(n)$ complexity.

The above mathematics underlies our proposed band matching method for a compact modeling of inductance and reluctance matrices. The key idea of our method is that we construct an approximate inductance matrix, denoted as $\tilde{L}$, whose band entries match those of the original L matrix, and whose inverse is banded.

A few observations of our band matching method can be made: (i) The physical meaning of inductance within the tridiagonal band of $\tilde{L}$ is preserved. (ii) $\tilde{L}$ is a Toeplitz matrix, which accurately reflects the uniform structure of the layout. (iii) It requires only $O(n)$ computation to construct $\tilde{L}$ and $\tilde{L}^{-1}$.

We prove in the next section that $\tilde{L}$ is guaranteed to be positive-definite whenever L is positive-definite.

III. Band matching method

In the preceding section, we used the example of tridiagonal reluctance matrices to illustrate the idea underlying our method. In practice, *banded* matrices with a bandwidth $2b+1$ are used (with tridiagonal matrices corresponding to the case $b = 1$) [5], [7], [3], [4], [16]. In the context of our band-matching method, this translates into constructing an approximate inductance matrix $\tilde{L}$, whose entries in the band of width $2b+1$ match those of L. In the following, we shall show that the techniques that we presented in Section II readily extend to the compact modeling of $\tilde{L}$ (and hence, $\tilde{L}^{-1}$). We will also formally prove that the resulting approximate $\tilde{L}$ is stable.

First, we generalize the definition of Hadamard product.

Definition 2: The Hadamard product of $X = [x_{i,j}^T]$ and $Y = [y_{i,j}]$ is defined by $X \circ Y = [x_{i,j}^T \times y_{i,j}]$, where $x_{i,j}, y_{i,j} \in R^b$.

For example, if the vectors u_1, u_2, v_1, and v_2 are of the same dimension b,

$$\begin{bmatrix} u_1^T & u_1^T \\ u_1^T & u_2^T \end{bmatrix} \circ \begin{bmatrix} v_1 & v_2 \\ v_2 & v_2 \end{bmatrix} = \begin{bmatrix} u_1^Tv_1 & u_1^Tv_2 \\ u_1^Tv_2 & u_2^Tv_2 \end{bmatrix}.$$

Next, we present the generalization of Lemma II.1:

Lemma III.1: ([11]) : Let $A \in R^{n,n}$ be symmetric, irreducible, and nonsingular. A has a bandwidth of $2b+1$ if and only if $B = [b_{i,j}] = A^{-1}$ is given by two sequences of vectors $\{u\}_{i=1}^n$, $\{v\}_{i=1}^n$, $u_i, v_i \in R^b$ such that

$$B = \begin{bmatrix} u_1^T & u_1^T & \cdots & u_1^T \\ u_1^T & u_2^T & \cdots & u_2^T \\ \vdots & \vdots & \ddots & \vdots \\ u_1^T & u_2^T & \cdots & u_n^T \end{bmatrix} \circ \begin{bmatrix} v_1 & v_2 & \cdots & v_n \\ v_2 & v_2 & \cdots & v_n \\ \vdots & \vdots & \ddots & \vdots \\ v_n & v_n & \cdots & v_n \end{bmatrix}.$$

Given B whose inverse has a bandwidth of $2b+1$, a set of corresponding parameterization vectors $\{u\}_{i=1}^n$, $\{v\}_{i=1}^n$, $u_i, v_i \in R^b$, can be computed as follows.

For $i \le b$:

$$u_i = e_i, \quad v_i = B(1:b,i).$$

For $b < i \leq n$:

$$u_i = \begin{bmatrix} v_i^T \\ v_{i-1}^T \\ \cdots \\ v_{i-b+1}^T \end{bmatrix}^{-1} \begin{bmatrix} B(i,i) \\ u_{i-1}^T v_i \\ \cdots \\ u_{i-b+1}^T v_i \end{bmatrix}$$

$$v_i = \begin{bmatrix} u_{i-2}^T \\ u_{i-1}^T \\ \cdots \\ u_{i-b-1}^T \end{bmatrix}^{-1} \begin{bmatrix} B(i-2,i) \\ B(i-1,i) \\ \cdots \\ B(i-b-1,i) \end{bmatrix}.$$

The parameterization of $\tilde{L}$ from L requires $O(nb^3)$ computation, where the $O(b^3)$ complexity is due to the $b \times b$ matrix inversions required. The construction of $\tilde{L}^{-1}$ from $\tilde{L}$ also required $O(nb^3)$ computation. Moreover, both $\tilde{L}$ and $\tilde{L}^{-1}$ can be compactly modeled with $O(nb)$ parameters. As $n >> b$, our proposed band matching method has linear time and space complexity.

In the remainder of this section, we prove the stability of our method. First, we introduce the notation and definitions used in the proof. We denote the minor formed from the rows $i_1, \cdots, i_k$ and columns $j_1, \cdots, j_k$ of A by $A\begin{pmatrix} i_1, & \cdots, & i_k \\ j_1, & \cdots, & j_k \end{pmatrix}$, where, $1 \leq i_1 < \cdots < i_k \leq n$, $1 \leq j_1 < \cdots < j_k \leq n$.

Definition 3: A matrix A is upper (lower) p-banded if $A_{ij} = 0$ for $j - i \geq p$ ($i - j \geq p$).

Definition 4: A matrix B has vanishing super-p-minors (sub-p-minors) if $B\begin{pmatrix} i_1, & \cdots, & i_p \\ j_1, & \cdots, & j_p \end{pmatrix} = 0$ for all indices that satisfy the condition $j_1 > i_p - p + 1$ ($i_1 > j_p - p + 1$).

The following two lemmas from [1] play an important role in proving the stability of our approximation.

Lemma III.2: ([1]) A nonsingular matrix A is upper (lower) p-banded if and only if A^{-1} has vanishing super-p-minors (sub-p-minors).

Lemma III.3: ([1]) If B is an $n \times n$ matrix with vanishing super-p-minors (sub-p-minors),

$$(d_1 d_2 \cdots d_{n-p}) \det B = D_1 D_2 \cdots D_{n-p+1}$$

where

$$d_k = B\begin{pmatrix} k+1, & \cdots, & k+p-1 \\ k+1, & \cdots, & k+p-1 \end{pmatrix},\ k = 1, \cdots, n-p,$$

$$D_k = B\begin{pmatrix} k, & \cdots, & k+p-1 \\ k, & \cdots, & k+p-1 \end{pmatrix},\ k = 1, \cdots, n-p+1.$$

We are now ready to prove the stability of our proposed method:

Theorem III.1: Suppose that L is positive definite. Then the matrix $\tilde{L}$ whose entries match those of L in the band of width $2b+1$, and whose inverse is $2b+1$-banded, is also positive definite.

Proof:

For any $n \times n$ matrix A, let A_m denote the $m \times m$ matrix in the top left-hand corner of A for $m = 1, \ldots n$. Then, a necessary and sufficient condition for $\tilde{L}$ to be positive definite is that $\det \tilde{L}_m > 0$ for $m = 1, \ldots n$; see for example, [14].

First consider the case when $m \leq b+1$. Then,

$$\det \tilde{L}_m = \det L_m > 0.$$

(The equality follows from the fact that the entries of $\tilde{L}$ match those of L in the band of width $2b+1$. The inequality follows from the positive definiteness of L.)

Now, consider the case when $m > b+1$. It is readily verified that as a consequence of the inverse $\tilde{L}$ being banded, the matrices $\tilde{L}_m$ are also parametrized by two sequences of vectors $\{u\}_{i=1}^m$, $\{v\}_{i=1}^m$, $u_i, v_i \in R^b$ such that

$$\tilde{L}_m = \begin{bmatrix} u_1^T & u_1^T & \cdots & u_1^T \\ u_1^T & u_2^T & \cdots & u_2^T \\ \vdots & \vdots & \ddots & \vdots \\ u_1^T & u_2^T & \cdots & u_m^T \end{bmatrix} \circ \begin{bmatrix} v_1 & v_2 & \cdots & v_m \\ v_2 & v_2 & \cdots & v_m \\ \vdots & \vdots & \ddots & \vdots \\ v_m & v_m & \cdots & v_m \end{bmatrix}.$$

From Lemma III.1, it follows that the matrix $\tilde{L}^{-1}$ is a banded matrix with bandwidth $2b+1$. From Lemma III.2, we obtain that $\tilde{L}_m$ has vanishing super- and sub-$(b+1)$-minors. Hence, by Lemma III.3

$$\det \tilde{L}_m = \frac{D_{m,1} D_{m,2} \cdots D_{m,m-b}}{d_{m,1} d_{m,2} \cdots d_{m,m-b-1}},$$

where

$$d_{m,k} = \tilde{L}_m\begin{pmatrix} k+1, & \cdots, & k+b \\ k+1, & \cdots, & k+b \end{pmatrix},\ k = 1, \cdots, m-b-1,$$

$$D_{m,k} = \tilde{L}_m\begin{pmatrix} k, & \cdots, & k+b \\ k, & \cdots, & k+b \end{pmatrix},\ k = 1, \cdots, m-b.$$

Note that $d_{m,k}$ and $D_{m,k}$ depend only on the band entries of $\tilde{L}_m$. As all the entries within the $2b+1$ band of $\tilde{L}$ are the same as the entries within the $2b+1$ band of L,

$$d_{m,k} = L_m\begin{pmatrix} k+1, & \cdots, & k+b \\ k+1, & \cdots, & k+b \end{pmatrix},\ k = 1, \cdots, m-b-1,$$

$$D_{m,k} = L_m\begin{pmatrix} k, & \cdots, & k+b \\ k, & \cdots, & k+b \end{pmatrix},\ k = 1, \cdots, m-b.$$

As L is positive definite, we have that all the $d_{m,k}$ and $D_{m,k}$ are positive [14]. Therefore $\det \tilde{L}_m > 0$, for the case $m > b+1$ as well, concluding the proof. □

IV. Experimental results

We consider a bus with 64 signals, with each wire of length 1mm and cross-section of $1\mu\text{m} \times 1\mu\text{m}$, and with a wire separation of 1μm. The wires were divided lengthwise into five segments. The driver resistance was assumed to be 30Ω and the load capacitance 40fF. HSPICE was used to obtain the simulation results.

A 1 V ramp input was applied to the first signal with the rest of the signals being quiet. We simulated the output from the first and second signals, using the $\bar{L}$ method [5], the window-based method [7], [3], [4], the wire duplication method [16], and finally the band-matching method described in this paper. The bandwidth that was used with all the method was seven. Simulation with the true L matrix (without any approximation) was used as the standard for comparison. All the approximate simulation methods took roughly the same time, as they enjoy the same sparsity in the reluctance matrix.

Figure 2 shows a plot of the errors in the voltages of the first signal using different method. Figure 4 shows the errors for the second signal. It is evident that all of the approximate methods yield comparable simulation accuracy.

V. Conclusion

We have presented an approach towards obtaining compactly-parametrized approximations to inductance matrices. Apart from acceptable approximation accuracy, the compact models also are provably stable. The work presented in this paper focuses on modeling wires in a single layer; the extension to multi-layer systems is currently under investigation.

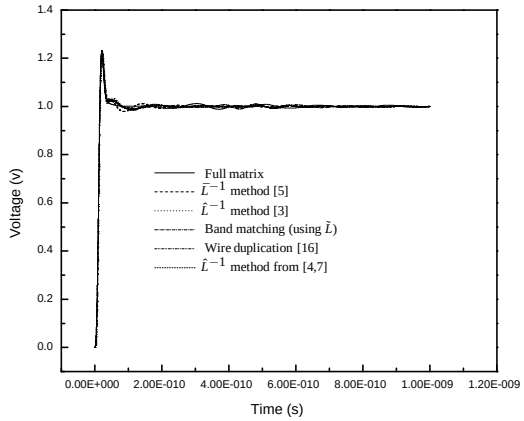

Fig. 1. Voltage on the first signal, simulated via the different methods.

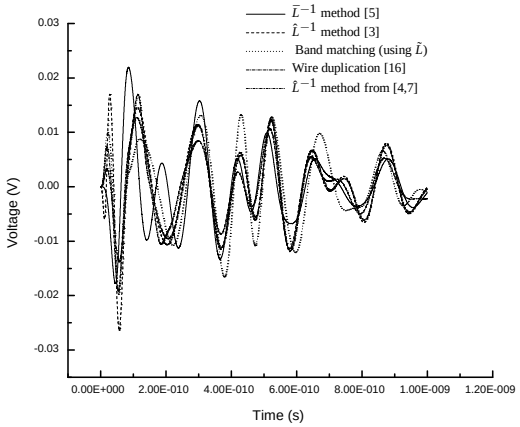

Fig. 2. Simulation error for the first signal voltage.

VI. Acknowledgment

The authors gratefully acknowledge financial support from National Science Foundation (CCR-9984553, CCR-0203362), a research grant from Purdue Research Foundation.

References

[1] W. W. Barrett and P. J. Feinsilver. Inverses of banded matrices. *Linear Algebra and its Applications*, 41:111–130, 1981.

[2] M. Beattie and L. Pileggi. Efficient inductance extraction via windowing. In *Proc. Design Automation and Test in Europe Conf.*, pages 430–436, 2001.

[3] M. Beattie and L. Pileggi. Modeling magnetic coupling for on-chip interconnect. In *Proc. Design Automation Conf*, pages 335–340, 2001.

[4] T. H. Chen, C. Luk, H. Kim, and C. C.-P. Chen. INDUCTWISE: Inductance-wise interconnect simulator and extractor. In *Proc. Int. Conf. on Computer Aided Design*, pages 215–220, 2002.

)(using L

matching

[3]Band

1method
[5] L

1method
Voltage (V)Time (s)fL

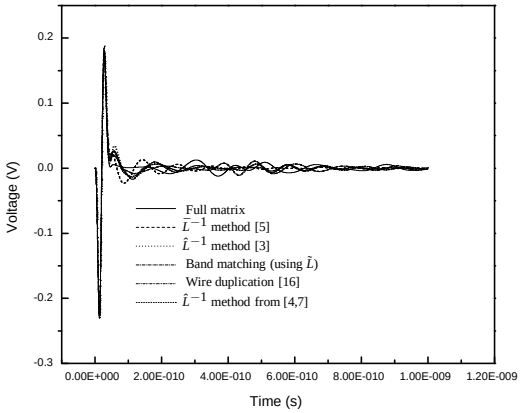

Fig. 3. Voltage on the second signal, simulated via the different methods.